Improvement of Pump Tubes for Gas Guns and Shock Tube Drivers

D. W. Bogdanoff*
NASA Ames Research Center, Moffett Field, California

In a pump tube, a gas is mechanically compressed, producing very high pressures and sound speeds. The intensely heated gas produced in such a tube can be used to drive light gas guns and shock tubes. Three concepts are presented that have the potential to allow substantial reductions in the size and mass of the pump tube and, possibly, modest but useful increases in sound speed to be achieved. The first concept involves the use of one or more diaphragms in the pump tube, thus replacing a single compression process by multiple, successive compressions. The second concept involves a radical reduction in the length-to-diameter ratio of the pump tube and the pump tube piston. The third concept involves shock heating of the working gas by high explosives in a cylindrical geometry reusable device. Preliminary design analyses are performed on all three concepts and they appear to be quite feasible. Reductions in the length and mass of the pump tube by factors up to ~11 and ~7, respectively, are predicted, relative to a benchmark conventional pump tube.

Nomenclature

A_b = barrel cross-sectional area, cm^2
a = acceleration of diaphragm, cm/s^2
c = sound speed, cm/s
c_o = initial sound speed in breech, cm/s
d = pump tube diameter, cm
f = a function
G = drive gas mass, gm
L_p = minimum allowable space between piston and unbroken diaphragm, cm
M = projectile mass, gm
p = pressure, dynes/cm^2
p_b = pressure to break diaphragm, dynes/cm^2
p_o = initial breech pressure, dynes/cm^2
T = temperature, °K
T_d = time for diaphragm to open, s
t = diaphragm thickness, cm
u_p = projectile muzzle velocity, cm/s
v = normalized volume of pump tube
v_d = opening velocity of diaphragm, cm/s
v_f = final pump tube volume, cm^3
v_p = piston velocity, cm/s
v_t = normalized total volume of pump tube
x_b = barrel length, cm

Greek

γ = specific heat ratio
π = 3.14159...
ρ = diaphragm density, gm/cm^3
σ_e = effective tensile strength of diaphragm, dynes/cm^2

Subscripts

1–8 = used to describe successive thermodynamic states in the pump tube cycles

I. Introduction

MECHANICAL compression and heating of a gas can be used to create reservoirs of hot, high-pressure gas. These reservoirs can then be used to accelerate a projectile or to drive a shock wave in a shock tube. A conventional technique of mechanical gas compression uses a free piston in a long tube. The piston is accelerated by a high-pressure gas or a powder charge in the "first stage" and then, in turn, compresses a gas in the "second stage". Very high pressures, temperatures, and sound speeds can be achieved in the second stage gas. These pump tubes are generally very long and massive relative to the rest of the apparatus. There also exist high explosive driven gas compressors that can create comparable gas reservoir conditions. These devices, in general, destroy themselves (and a considerable fraction of their immediate surroundings) upon use. In this paper, three techniques are examined, which have the potential, in reusable devices, for the achievement of substantial reductions in pump tube sizes and masses. These techniques may also, under some circumstances, have the potential for the achievement of higher gas sound speeds. The following paragraphs describe the operation of a conventional pump tube (that of a two-stage light gas gun), which is then used as a benchmark to assess the potential of the proposed techniques.

A representative two-stage light gas gun operates as follows. A powder charge is burned at one end of a large, long pump tube, accelerating a relatively heavy piston to velocities typically in the range 0.5–1.0 km/s. The piston compresses a working gas, usually hydrogen, producing pressures of thousands of atmospheres and temperatures estimated at several thousand degrees Kelvin. This reservoir of hot, high-pressure gas then accelerates the relatively small projectile in the gun barrel, which is attached to the end of the pump tube. Frequently, a burst diaphragm is placed just behind the projectile, so that it does not start to accelerate until the pump tube pressure becomes fairly high. Further details are given in Refs. 1 and 2.

Guns of this type can fairly routinely achieve velocities of 7–8 km/s; by using very light projectiles and stressing the gun severely, velocities up to 11–12 km/s can be achieved.[2] To obtain still greater velocities using the conventional two-stage gun configuration is very difficult. Increasing the length and/or the diameter of the pump tube, thereby presumably increasing the volumetric compression of the gas, and preheating of the pump tube gas before compression

---

Received Aug. 1, 1988; revision received March 3, 1989.

*Senior Research Scientist, Aerothermodynamics Branch. Member AIAA.

have both been tried, yielding little or no gain in projectile velocity.[3]

The pump tube of a two-stage light gas gun is very massive and long relative to the barrel. For example, for the 2.54 cm (barrel diameter) gun at the NASA Ames Research Center, the pump tube diameter is 4 times the barrel diameter, and the pump tube length is about 3.4 times the barrel length. (The diameters quoted above are inside diameters.) The pump tube is 23 meters long, based on the initial length of the working gas, and ~25 meters long overall. A reduction in pump tube length and mass, while maintaining gun performance, would be very desirable. In this paper, three modifications of the conventional pump tube configuration are proposed, with a view to reduction in pump tube size and/or increase in sound speed obtained. (These modifications may also be applied to pump tubes used as drivers for shock tubes and shock tunnels.) The first modification involves the insertion of a diaphragm into the pump tube to divide the single gas compression operation into two (or more) such operations. The second modification involves a radical reduction in the length-to-diameter ratio of the pump tube and the pump tube piston. The third modification involves shock heating using high explosives in a reusable device. These modifications are discussed in more detail below.

II. Pump Tube Diaphragm

A conventional two-stage light gas gun and a gun including a pump tube diaphragm are shown schematically in Figs. 1a and 1b. It is recognized that conventional pump tubes frequently have additional complexities, such as special shaping of the front of the pump piston and tapering at the end of the pump tube, as shown in Fig. 1c. No attempt will be made here to analyze the additional complexities of the compression process introduced by these features. All analyses made here will be made with respect to the simplified pump tubes shown in Figs. 1a and 1b.

The basic advantage of using the pump tube diaphragm is as follows. Let a volumetric compression of the pump tube gas of 100 to 1 be required to achieve the necessary final gas temperature, using the conventional pump tube. Let the final pump tube volume be v_f; the initial pump tube volume must then be $100v_f$ for the preceding case. Using the pump tube diaphragm, the first compression could compress the gas from $10v_f$ to v_f. The diaphragm would then break and the gas would expand into the vacuum region without loss of temperature, since it does no work (ignoring the small amount of work required to break the diaphragm). The already hot gas is then compressed again from $10v_f$ to v_f, reaching, ideally, the same temperature achieved in the conventional pump tube. However, the total pump tube volume for the second case is only about $20v_f$ or about 5 times less than that of the conventional pump tube. Conversely, if a pump tube of volume $100v_f$ were divided into two $50v_f$ volumes and each section of the pump tube was compressed to v_f in succession by the piston, the effective volumetric compression would be $50^2 = 2500$ to 1 instead of 100 to 1, if the pump tube were operated in the usual way. Assuming an ideal gas, no losses, and taking the specific heat ratio to be 1.4, this would allow the pump tube with the diaphragm to achieve a final sound speed $(2500/100)^{(1.4-1)/2} = 1.903$ times that of the pump tube without the diaphragm.

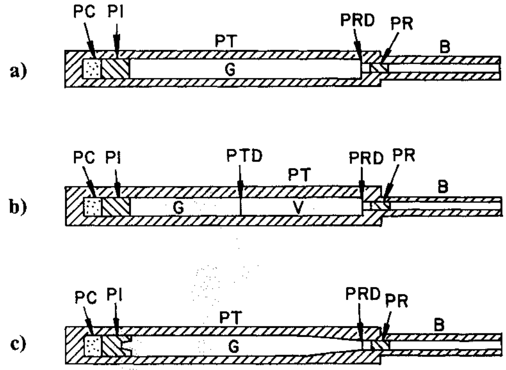

Fig. 1 Conventional two stage light gas guns, (a) and (c), and a gun with a pump tube diaphragm (b). PT denotes pump tube, B, barrel, PC, powder charge, PI, piston, PR, projectile, PRD, projectile diaphragm, G, pump tube gas, V, vacuum, and PTD, pump tube diaphragm.

The above calculations will now be repeated in more detail and tied to experimental results for the benchmark conventional pump tube case. The pump tube gas is assumed to be thermally and volumetrically perfect, with a constant specific heat ratio of 1.4. There are no heat transfer losses and the work of breaking diaphragms is neglected. The kinetic energy of the pump tube gas is ignored. This is equivalent to assuming that the Mach number of the pump tube gas is small. This is not too bad an assumption, because the pump tube gas is hydrogen, with an initial sound speed of ~1.3 km/s, which increases upon compression, and typical piston velocities for the benchmark pump tube modelled[4] are ~0.7 km/s. In estimating the velocity reached by the projectile, the difference between the pump tube diameter and the barrel diameter is ignored. The compression cycle(s) of the pump tube is considered to be completed, with the piston at rest, just before the projectile diaphragm breaks and the projectile starts to accelerate. These assumptions obviously lead to a very simplified picture of gun operation, but, in general, the resulting errors in performance prediction should occur in similar ways for both the conventional gun and the gun with the pump tube diaphragm. Hence, the large differences in the predicted sizes and performances of the various pump tubes to the discussed below should be realizable, to a considerable extent, in reality, despite the simplicity of the analysis.

The benchmark conventional gun case modelled is one particular shot of the 2.54 cm diameter gun at the NASA Ames Research Center. The parameters for this shot are given in Table 1. To carry out the simplified theoretical analysis, it is necessary to have an estimate for the maximum pressure in the pump tube. In reality, the end of the pump tube compression process and the beginning of the acceleration of the projectile in the barrel overlap in time and are not separated, as in the present simple theory. Measured second-stage pressures from Ref. 5 show a period of relatively constant pressure at the beginning of the projectile acceleration, rather than anything like the ideal peak followed by a steep, smooth falloff. We have made no attempt to model this complex compression and acceleration process. Rather, an effective maximum gas pressure was estimated as follows. A guess is first made for the maximum gas pressure. With our simplifying assumptions, all gas conditions at the end of the compression process can then be calculated. Figure 2, adapted from Ref. 6, gives calculated curves for projectile velocity for a gun with an ideal working gas with specific heat ratio (γ) of 1.4

Table 1 Experimental parameters for shot in 2.54 cm gun

Date	16 Oct. 1987
Round number	1761
Barrel diameter	2.54 cm
Pump tube diameter	10.16 cm
Barrel length	731 cm
Pump tube length (filled with gas)	2344 cm
Pump tube initial gas pressure	3.45×10^6 dynes/cm^2
Mass of gas	52.56 g
Mass of piston	7260 g
Piston velocity	0.742×10^5 cm/s
Projectile diaphragm break pressure	3.45×10^8 dynes/cm^2
Projectile mass	13.22 g
Projectile muzzle velocity	6.61×10^5 cm/s

and no difference between the breech (pump tube) diameter and the barrel diameter. The data of Fig. 2 is presented in the form of curves of $u_p/c_o = f[(p_o A_b x_b)/(Mc_o^2)]$, with G/M as a parameter varying among the curves. The variables are defined in the nomenclature. (We note here that we have changed the notation of Ref. 6 slightly.) From these curves, we can then estimate the projectile muzzle velocity. The guessed value of the maximum gas pressure is then iterated until the predicted and measured projectile velocities are in agreement. The pressure thus found was 6.90×10^9 dynes/cm^2.

With this estimate for the effective maximum gas pressure, Table 2 can be constructed, giving the state variables at various points in the cycles for the conventional pump tube ("single compression pump tube") and the pump tube with the diaphragm ("double compression pump tube"). At this point, it is well to make a diversion to comment on the accuracy of the quantities in Table 2 (and also in Tables 3–6 and 8). The calculations are made with many simplifying assumptions, and errors of 20 or 30% or more would be expected. We have chosen not to reflect these large errors by using fewer significant figures in the tables because important differences would tend to be obscured. For the single compression pump tube, the two state points are at the beginning and the end of the piston stroke, respectively. For the double compression pump tube, the four state points are, in order, at

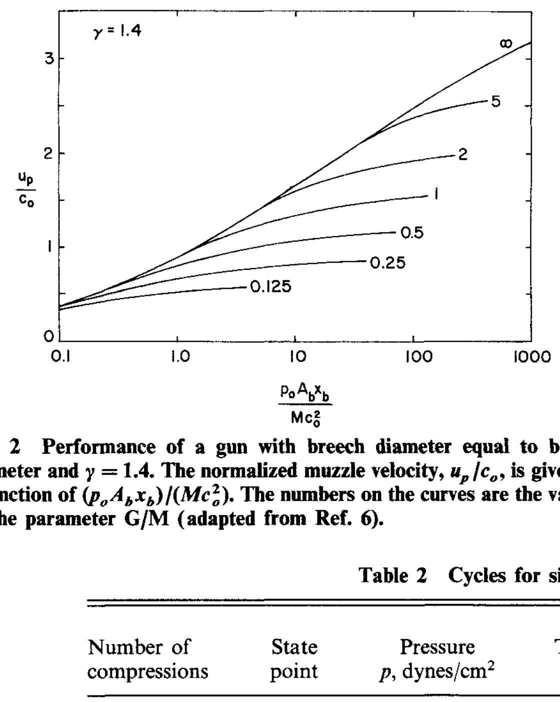

Fig. 2 Performance of a gun with breech diameter equal to barrel diameter and $\gamma = 1.4$. The normalized muzzle velocity, u_p/c_o, is given as a function of $(p_o A_b x_b)/(Mc_o^2)$. The numbers on the curves are the values of the parameter G/M (adapted from Ref. 6).

the beginning of the piston stroke, just before the diaphragm ruptures, just after the diaphragm ruptures but with the gas expanded to fill the remaining pump tube space, and at the end of the piston stroke. For the single compression pump tube, p_1 is the given experimental value, p_2 is estimated as described earlier, and T_1 is assumed to be 300°K. All the remaining variables are calculated assuming an isentropic compression of an ideal gas. The volume is normalized to the volume at the end of the piston stroke. To obtain a comparable double compression pump tube case, we assumed, first, that the final gas state is identical to that achieved by the single compression pump tube; second, that the initial temperature is 300°K; third, that the two compressions were volumetrically by equal factors; and, last, that the volume at the end of the first compression is the same as that at the end of the second compression. The expansion from state 2 to state 3 is at constant internal energy. With these assumptions, the state variables given in the second part of Table 2 for the double compression pump tube can be calculated.

The normalized volume v is the volume actually occupied by the gas at each state. The total normalized volume v_t is the volume between the head of the piston and the projectile end of the pump tube at the moment each state is achieved. For the double compression pump tube, this includes the evacuated volume during the first part of the compression process. The total pump tube volume required is proportional to the maximum value of v_t, as long as the final volume is kept constant, which is true for all cases discussed, except for one case in Table 6. From Table 2, we can see that the required pump tube volume (to achieve the same final conditions) is 7.8 times smaller, using the double compression pump tube vs the conventional single compression pump tube. A similar calculation can be made for a triple compression pump tube. The additional reduction in pump tube volume in going from a double to a triple compression pump tube is, however, only by a factor of ~1.8, and the complexity would be greater.

There are several difficulties in translating the double compression pump tube shown in Table 2 into reality. First, it is likely that a practical double compression pump tube will use a deformable piston impacting a tapered section at the end of the pump tube, as does the benchmark conventional pump tube. Hence, the second compression will probably be greater volumetrically than the first compression, in contrast to the case shown in Table 2. Second, there are two difficulties with conditions at the end of the first compression in the case shown in Table 2. We assume that the diaphragm is to be opened by the gas pressure alone and is to be completely clear of the piston by the time the latter passes. One can readily

Table 2 Cycles for single and double compression pump tubes

Number of compressions	State point	Pressure p, dynes/cm^2	Temperature T, °K	Sound speed c, cm/s	Normalized volume v	Total normalized volume v_t
1	1	3.50×10^6	300	1.32×10^5	228	228
1	2	6.90×10^9	2630	3.90×10^5	1	1
2	1	5.20×10^7	300	1.32×10^5	15.1	15.1
2	2	2.33×10^9	890	2.27×10^5	1	15.1
2	3	1.54×10^8	890	2.27×10^5	15.1	15.1
2	4	6.90×10^9	2630	3.90×10^5	1	1

Table 3 More practical double compression pump tube cycle

Number of compressions	State point	Pressure p, dynes/cm^2	Temperature T, °K	Sound speed c, cm/s	Normalized volume v	Total normalized volume v_t
2	1	3.20×10^7	300	1.32×10^5	24.4	58
2	2	4.00×10^8	620	1.90×10^5	4	37
2	3	4.30×10^7	620	1.90×10^5	37	37
2	4	6.90×10^9	2630	3.90×10^5	1	1

estimate (using the techniques of Sec. III) that, for the small normalized volume v_2 shown in Table 2, and typical piston velocities, there is insufficient time for the diaphragm to get out of the way. Also, the break pressure for the pump tube diaphragm ($\simeq p_2$ in Table 2) is very high and the diaphragm, therefore, must be correspondingly thick. Even if there was sufficient time for the diaphragm to open as far as it was going to, with a very thick diaphragm it is possible that parts of the diaphragm would not completely clear the piston path. If this were to happen, since the diaphragm is thick and robust, substantial damage to the piston could occur as it passes the diaphragm station.

The difficulties discussed above are addressed by making two simple, somewhat arbitrary changes from the double compression pump tube cycle of Table 2. First, v_3/v_4 is made equal to $(v_1/v_2)^2$ instead of (v_1/v_2). Second, v_2 is made equal to $4v_4$ instead of v_4. With these two changes, and otherwise following the calculation techniques discussed earlier, we can arrive at the more practical double compression pump tube cycle shown in Table 3. Note that p_2 is now sufficiently low to make the pump tube diaphragm practically thin, and v_2 is sufficiently large to allow time for the diaphragm to get out of the way. (Further details are given in Sect. III.) The maximum pump tube volume for the more practical case of Table 3 is about twice that of the double compression gun case of Table 2, but still 3.9 times less than that of the conventional single compression gun.

The maximum pump tube gas volume extends from the front of the piston, in its initial position, to the projectile diaphragm. Behind this volume is the piston, the powder chamber, and the breech block. If these latter components do not change in the comparison between the single and double compression pump tubes, a reduction in maximum pump tube gas volume by a factor of 3.9, as calculated above, translates into a somewhat smaller reduction in total pump tube length. Using the dimensions for the NASA Ames 2.54 cm gun, the reduction in maximum pump tube gas volume by a factor of 3.9 corresponds to a reduction in overall pump tube length by a factor of about 3.2. If the gun barrel remains unchanged in the comparison between the two guns, the reduction in overall gun length will be by a still smaller factor. Again using dimensions of the NASA Ames 2.54 cm gun, the corresponding reduction in overall gun length is by a factor of about 2.2. With this length reduction, in a given facility length, using double vs single compression would allow, in principle, the use of a gun with a caliber larger by a factor of 2.2.

In principle, multiple compression technique can also be used to obtain a higher performance from a given pump tube. Table 4 shows calculated cycles for double and quadruple compression guns configured to give higher performance from a given pump tube. The cycles of Table 4 are referenced, as before, to the conventional single compression cycle of Table 2. The intermediate maximum volumes for each of the two cases of Table 4 were taken to be equal. In the cases of Table 4, we have gone directly to realistic cycles in that the intermediate minimum volumes are 4 times the final minimum volume. Thus, the final compressions are greater volumetrically than the preceding compressions and the minimum volumes are large enough to allow the diaphragms enough time to open sufficiently to get out of the way of piston. Table 4 predicts, ideally, very high temperatures and sound speeds at the end of the compression process.

Using the conditions at the end of the compression processes in Table 4 and the corresponding benchmark conditions for the conventional single compression pump tube from Table 2, projectile velocities may be calculated using the curves of Ref. 6 as described earlier. The results of these calculations are given in Table 5. The velocities in Table 5 were calculated for two projectile masses. The first mass is 13.22 g, that actually used in the benchmark shot of Table 1. This represents a fairly routine operating mode of the conventional single compression gun, not attempting to reach extremely high velocities. The second mass is one-third of the first mass, and represents an attempt to push the guns towards the maximum attainable velocities. From Table 5, ideally, substantial increases in projectile velocity are predicted through the use of the multiple compression technique.

Unfortunately, there are a number of arguments, both theoretical and experimental, that indicate that the ideal velocity gains shown in Table 5 may be very difficult to achieve in practice. For the multiple compression pump tube cycles shown in Tables 2 and 3, the gas temperatures reached are no higher than in the corresponding single compression pump tube and the time for the stroke of the piston would be much shorter than that for the single compression pump tube. Hence, one may reasonably argue that heat transfer losses should be no larger and might even be smaller in the multiple compression pump tube, compared to those in the single compression pump tube. However, for the multiple compression cycles of Table 4, the gas temperatures are much higher than those for the corresponding single compression pump tube and the piston stroke times are the same between the corresponding multiple and single compression pump tube cases. Hence, the heat transfer losses, particularly radiation, are likely to be very much larger for the multiple compression cases. Also, with the very high temperatures of the multiple compression cases, it is likely that there will be an increase in ablation of the pump tube and barrel material and incorporation of the ablated material into the working gas. This could lead to an increase in the mean molecular weight of the pump tube working gas and a corresponding tendency for the gas sound speed and the projectile muzzle velocity to decrease, as the gas temperature is raised using multiple compressions. Finally, as mentioned earlier, experimental attempts to increase projectile velocities by preheating the pump tube gas or by increasing the volume of the pump tube, thereby pre-

Table 4 Multiple compression cycles for obtaining higher performance from a given pump tube

Number of compressions	State point	Pressure p, dynes/cm^2	Temperature T, °K	Sound speed c, cm/s	Normalized volume v	Total normalized volume v_t
2	1	2.31×10^6	300	1.32×10^5	116	228
2	2	2.58×10^8	1150	2.59×10^5	4	116
2	3	8.90×10^6	1150	2.59×10^5	116	116
2	4	6.90×10^9	7700	6.70×10^5	1	1
4	1	8.70×10^5	300	1.32×10^5	60	228
4	2	3.80×10^7	890	2.27×10^5	4	172
4	3	2.56×10^6	890	2.27×10^5	60	172
4	4	1.13×10^8	2620	3.90×10^5	4	116
4	5	7.60×10^6	2620	3.90×10^5	60	116
4	6	3.40×10^8	7700	6.70×10^5	4	60
4	7	2.24×10^7	7700	6.70×10^5	60	60
4	8	6.90×10^9	40000	15.20×10^5	1	1

Table 5 Calculated projectile velocities for guns with different numbers of compressions

Number of compressions	Projectile mass, g	Projectile velocity, cm/s	Normalized projectile velocity
1	13.22	6.7×10^5	1.0
2	13.22	8.6×10^5	1.29
4	13.22	9.7×10^5	1.45
1	4.407	8.3×10^5	1.0
2	4.407	11.7×10^5	1.41
4	4.407	15.8×10^5	1.90

Table 6 Double and single compression cycles for mode 3 use in a shock tube

Number of compressions	State point	Pressure p, dynes/cm^2	Temperature T, °K	Sound speed c, cm/s	Normalized volume v	Total normalized volume v_t
1	1	3.40×10^6	300	1.32×10^5	228	228
1	2	6.90×10^9	2630	3.90×10^5	1	1
2	1	3.80×10^6	300	1.32×10^5	205	228
2	2	2.63×10^8	1000	2.42×10^5	10	33
2	3	7.90×10^7	1000	2.42×10^5	33	33
2	4	2.30×10^9	2630	3.90×10^5	3	3

sumably increasing the volumetric compression of the pump tube gas, have met with little or no success.[3] Since our multiple compression technique is a kind of preheating, these experimental observations do not augur well for the use of the multiple compression technique to attempt to increase the performance of a given pump tube. From the above discussion, it appears that, for guns, the theoretical benefits of the multiple compression technique are more likely to be translatable into reality when used in the mode of obtaining the same sound speed with a shorter pump tube (Mode 1—cases in Tables 2 and 3) than in the mode of obtaining a higher sound speed with a given pump tube (Mode 2—cases in Table 4). However, the multiple compression technique discussed here is different from the techniques discussed in Ref. 3, which were found to yield little projectile velocity gains, and it may be possible that it could, in reality, yield some modest, but useful, projectile velocity gains.

The multiple compression technique can also be applied to piston-driven shock tubes or shock tunnels. Mode 1 could be used to obtain the same driver conditions with a shorter pump tube. Mode 2 could, in principle, be used to obtain higher driver sound speeds with a given pump tube. The caveats discussed above with respect to the realization of the mode 2 performance gains in guns in reality must be borne in mind. However, these may not be as severe for shock tubes as for guns, for the following reason. For guns, after the compression process, the gas remains in the very hot, compressed state for a relatively long time, due to the inertia of the projectile as it accelerates in the barrel. During this time, heat transfer losses and ablation are likely to be severe. However, in a shock tube or shock tunnel, once the compression is completed and the diaphragm breaks, the gas expands and the temperatures drop relatively rapidly. With this rapid expansion in the shock tube relative to that in the gun, the duration of the very high temperatures in the former is significantly shorter than in the latter and, thus, heat transfer and ablation problems should be less severe in the former case. Hence, mode 2 may be more useful when used with a shock tube than with a gun.

In a shock tube or shock tunnel, it may be desirable to employ the multiple compression technique in a third mode (Mode 3). In this mode, with a given pump tube, multiple compression is used to achieve the same temperature as with the reference single compression case, but with a larger final volume. Mode 3 can thus be used to increase the final clearance between the piston and the end of the pump tube. Table 6 shows cycles for single and double compression, using the mode 3 multiple compression technique to increase the final volume while using the same pump tube and maintaining the final temperature achieved. The reference single compression case is the same one presented in Table 2. In Table 6, v_2 and v_4 for the double compression case were somewhat arbitrarily chosen to be 10 and 3, respectively, and p_4 was chosen so that the product p_4v_4, which is proportional to the total gas energy, was the same for the single and double compression cases. The double compression case of Table 6 is somewhat different from all the preceding multiple compression cases, in that p_4 and v_4 are not the same as the values for the corresponding single compression case. If the final total gas energy is kept constant, the increase in piston clearance is accomplished at the cost of a proportionate reduction in final gas pressure. It may be feasible to consider some recovery of final gas pressure (after its reduction through the application of the multiple compression technique) by raising all of the cycle pressures.

III. Diaphragm Operation and Sizing

Figure 3 shows a sketch of one possible method of installing the pump tube diaphragm. Gas seals, diaphragm gripping ridges, etc., are not shown for clarity. A taper is provided to guide the projectile into the second tube. The open diaphragm position is shown dashed. We now outline a very simple method of estimating the diaphragm opening time. When this time estimate is combined with the piston velocity, a minimum acceptable volume at the end of an intermediate compression process is defined. The diaphragm is considered to accelerate at a constant rate from an initial planar configuration, driven by a constant gas pressure p_b. The increase of the gas pressure due to piston motion and the subsequent decrease of gas pressure due to diaphragm rupture are not considered. The material of the center of the diaphragm becomes that at the tips of the petals and is assumed to have to move through an arc of length

$$s = \frac{\pi d}{4} \tag{1}$$

to get out of the way of the piston, where d is the pump tube diameter. The acceleration of the diaphragm a is given by

$$a = \frac{p_b}{\rho t} \tag{2}$$

where p_b is the diaphragm break pressure, ρ is the diaphragm density, and t is the diaphragm thickness. The time for the diaphragm to open, T_d, that is, the time for the center of the diaphragm to travel the distance s, is given by

$$T_d = (2s/a)^{1/2} = \left(\frac{\pi d \rho t}{2p_b}\right)^{1/2} \tag{3}$$

We can relate p_b to be effective tensile strength of the diaphragm σ_e by

$$p_b = \frac{4\sigma_e t}{d} \tag{4}$$

Combining Eqs. (3) and (4), we obtain

$$T_d = d\left(\frac{\pi\rho}{8\sigma_e}\right)^{1/2} \tag{5}$$

We define the opening velocity of the diaphragm v_d as

$$v_d = \frac{\pi d}{4T_d} = \left(\frac{\pi\sigma_e}{2\rho}\right)^{1/2} \tag{6}$$

where v_d is seen to be dependent only upon σ_e and ρ. By combining Eqs. (5) and (6), we can obtain

$$T_d = \frac{\pi d}{4v_d} \tag{7}$$

The minimum allowable clearance distance between the piston and the unbroken diaphragm, L_p, is given by

$$L_p = v_p T_d \tag{8}$$

where v_p is the piston velocity. We can combine Eqs. (7) and (8) to obtain

$$\frac{L_p}{d} = \frac{\pi v_p}{4v_d} \tag{9}$$

Effective tensile strength data for 1100-0 aluminum and annealed 304 stainless steel were obtained from Refs. 7 and 4, respectively. These data were for actual breakage of diaphragms in configurations similar to those proposed here and, hence, include the weakening effect of the diaphragm scoring. The σ_e values for the two materials were 5.32×10^8 and 2.21×10^9 dynes/cm^2, respectively, considerably below the handbook values, showing the effect of diaphragm scoring. From these values and the densities of the two materials, the diaphragm (opening) velocities can be calculated from Eq. (6). We take a typical piston velocity[4] as that of the NASA Ames 2.54 cm gun, ~0.7 km/s. Using this value as v_p in Eq. (9), we obtain L_p/d, the required minimum clearances for the piston (normalized by the pump tube diameter), at the time the diaphragm begins to open. These values, along with the diaphragm velocities and other relevant parameters, are given in Table 7 for the two diaphragm materials. For the realistic multiple compression cycles presented in Tables 3, 4, and 6, the highest pressure at the end of an intermediate compression is 4.05×10^8 dynes/cm^2. Using this value and the σ_e values of the two candidate diaphragm materials, from Eq. (4) we can calculate the necessary diaphragm thickness (normalized by the pump tube diameter), t/d. These values are also given in Table 7.

For the realistic multiple compression cycles presented in Tables 3, 4, and 6, we can use the values of the complete pump tube volume at the beginning of the cycle v_{t1}, the gas volume at the end of the intermediate compression (v_2 and, for the four compression case, v_4 and v_6), and the dimensions of the pump tube from Table 1, to calculate the values of L_p/d actually obtained in the proposed cycles at the end of the intermediate compressions. These values are between 4 and 10, which are greater than both limiting values shown in Table 7. Hence, based on the preceding simple model for diaphragm opening, the realistic multiple compression cycles of Tables 3, 4, and 6 do allow enough time for the diaphragm to open and get out of the way. From Table 7, the necessary normalized thickness of the aluminum diaphragm is rather large. For the high pressure for which the t/d values of Table 7 were calculated, it would be better to use stainless steel diaphragms, which have a very reasonable normalized thickness.

Summing up, the necessary pump tube diaphragms appear to open sufficiently fast and to be not unreasonably thick. In an experimental proof of concept of the multiple compression technique, pump tube diaphragm performance must be carefully monitored, to be sure that they do, in fact, open fast enough and fully, do not damage the piston, and do not send any significant or damaging fragments down the tube.

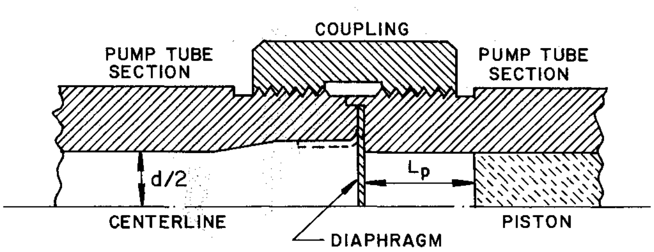

Fig. 3 Installation of diaphragm in pump tube. Gas seals, diaphragm gripping ridges, etc., are omitted for clarity. Open position of diaphragm is shown dashed.

IV. Low-Aspect Ratio Pump Tube

We will again use the Ames 2.54 cm gun as a benchmark. The overall pump tube length is ~25 m. The pump tube inside diameter is 10.16 cm. The actual overall length of the pump tube piston is 1.016 m. The pump tube has a conical depression in its forward face (see Fig. 1c). The effective piston length, for the same mass, if the piston were a solid cylinder with flat ends, is 0.982 m. The aspect ratio of the piston, using the effective length, is 0.982/0.1016 = 9.67. Reference 8 indicates that projectiles with aspect ratios as low as 0.431 have been successfully fired in guns. If the aspect ratio of the piston is changed from 9.67 to 0.431, keeping the same mass, the piston diameter becomes 28.65 cm and its length 12.35 cm. The piston diameter has been increased by a factor of 2.82 and the piston length has been reduced by a factor of 7.95. The benchmark piston and pump tube and the low aspect ratio piston and pump tube are shown in Fig. 4.

It should be possible to reduce the pump tube length by a factor close to that by which the piston is reduced. If, for purposes of illustration, we use exactly the same factor, the pump tube length could be reduced from ~25 m for the benchmark gun to 3.1 m for the low-aspect ratio gun. Since

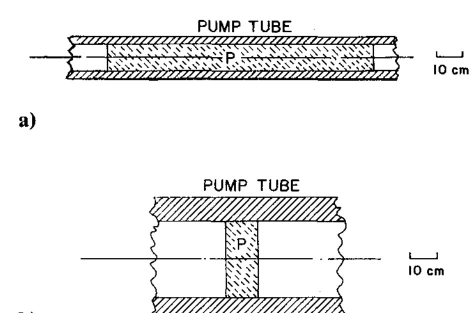

Fig. 4 Conventional (a) and low aspect ratio (b) pistons (P) in pump tubes. Fig. 4a shows the piston and pump tube of Ames' 2.54 cm gun.

Table 7 Pump tube diaphragm characteristics

Material	Reference number	Effective tensile strength, dynes/cm^2	Density, g/cm	Diaphragm velocity, cm/s	L_p/d	t/d
1100-0 aluminum	7	5.32×10^8	2.7	1.75×10^4	3.13	0.191
304 stainless steel	4	2.21×10^9	7.6	2.14×10^4	2.57	0.046

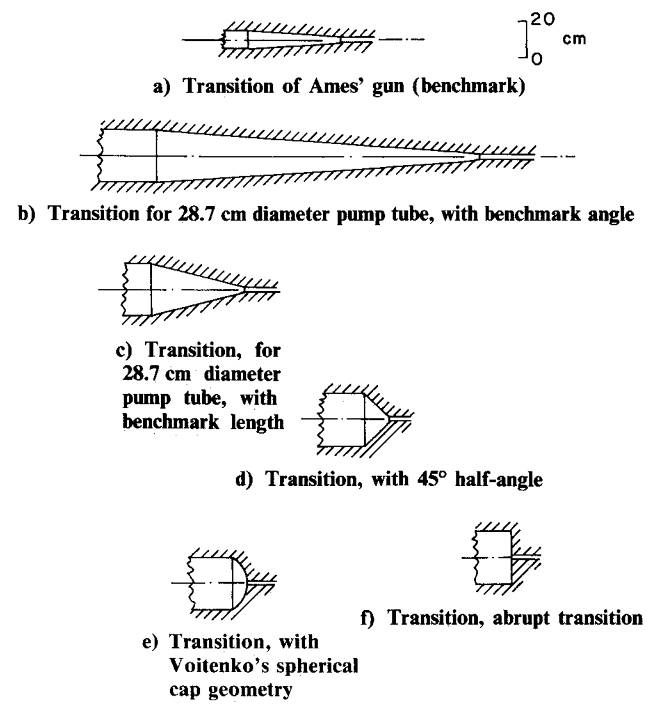

Fig. 5 Possible geometries for transition from pump tube to 2.54 cm diameter barrel.

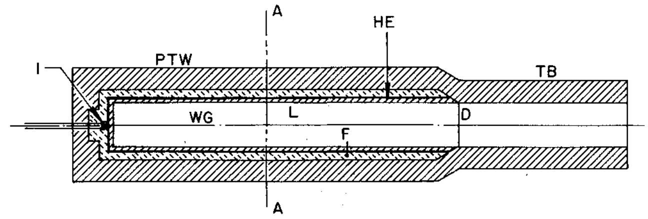

Fig. 6 Reusable high-explosive shock-heated pump tube. PTW denote pump tube wall, F, cushioning foam (or vacuum standoff region), HE, high explosive, L, metal liner, WG, working gas, I, initiator, D, diaphragm and TB, driven (shock) tube or gun barrel. The radial dimensions along line AA are to scale. The axial dimensions are not to scale with respect to the radial dimensions. The HE is indicated by the thick black line.

the two pump tubes enclose the same volume of gas and should have roughly the same operating pressures, the masses of the two pump tubes should be roughly equivalent. The advantage of the low-aspect ratio pump tube is shorter length, not smaller mass. The low-aspect ratio pump tube should also have smaller gas frictional and heat transfer losses, since its surface-to-volume ratio is superior and the piston stroke time is smaller, assuming the same piston velocity.

Some possibilities for the transition from the pump tube to the barrel are shown in Fig. 5a, showing the transition section of the benchmark gun. Figures 5b through 5f show some possible transition sections for the gun with the low-aspect ratio pump tube. The transition section might be made using either the angle (Fig. 5b) or the length (Fig. 5c) of the transition section of the benchmark gun. Conical transition sections with still steeper angles might be used (Fig. 5d), as could Voitenko's[9] spherical cap geometry (Fig. 5e). An abrupt transition (Fig. 5f) could also be made. No attempt is made here to choose among the geometries of Figs. 5b–f. They are discussed briefly only to point out that this is a critical area for the development of a gun with a low-aspect ratio pump tube.

The low-aspect ratio pump tube has been estimated to be shorter by a factor of 7.95 than the benchmark pump tube. We assume that a 2.54 cm gun is constructed using the low-aspect ratio pump tube, a transition section with the same length as that of the benchmark gun (e.g., see Fig. 5c) and the barrel of the benchmark gun. The overall length of this gun is 11.8 m vs 33.3 m for the benchmark gun; the reduction in overall gun length is by a factor of 2.8.

We assume that the piston of the low aspect ratio pump tube is made of the same material (polyethylene) and moves at the same velocity ($\sim$0.7 km/s) as for the benchmark gun. If the piston impacts normally on the steel, the maximum stress can be estimated readily, using a linear acoustic analysis. (Such an impact might occur in the geometry of Fig. 5f if there was no gas initially in the pump tube.) The stress obtained in this way is 1.26×10^{10} dynes/cm^2. From Ref. 10, the yield strengths of 4130 steel heat treated to Brinell hardnesses of 315, 380, and 435 are 0.91×10^{10}, 1.19×10^{10}, and 1.38×10^{10} dynes/cm^2, respectively. The respective elongation values are 17%, 13%, and 11%. The above numbers and the success of the Ames benchmark gun and other guns using similar piston materials and velocities suggest that a transition section with a reasonably long life can be designed for a gun with a low-aspect ratio pump tube.

V. Shock Heating with High Explosives

References 11–13 report one-shot (expendable) devices driven by detonations in high explosives. These pump tubes were applied both as shock tube and light-gas gun drivers. Shock velocities of 14-18 km/s and projectile velocities up to $\sim$6 km/s (for projectile masses of 4 to 100 g) were obtained. Figure 6 shows a proposed reusable version of the pump tube driver of Refs. 11–13. The operation of this type of driver is discussed in detail in the above references and will be outlined only briefly here.

On initiation of the HE charge, the detonation wave proceeds out from the initiator and down the annular HE charge. This drives the metal liner inwards behind the detonation wave, forming a conical piston that moves through the working gas at the detonation velocity. This piston drives a shock through the working gas. The shock moves at a velocity somewhat higher than the detonation velocity. The gas is compressed and intensely heated by the shock wave in a strongly nonisentropic process. In some geometries, such as that of Fig. 6, the initial shock can be reflected by an area contraction, further compressing and heating the gas. A diaphragm can be placed at the end of the pump tube to release the compressed gas at the desired pressure. Beyond the diaphragm, one may have either the driven tube of a shock tube or a gun barrel containing a projectile.

It is proposed to make the pump tube driver reusable, in contrast to those of Refs. 11-13, by the following techniques. First, the amount of high explosive is reduced significantly. Second, a strong steel vessel surrounds the HE charge. Third,

Table 8 High-explosive driven shock compression cycle

State point	Pressure p, dynes/cm^2	Temperature T, °K	Sound speed c, cm/s	Normalized volume v
1	1.22×10^7	300	1.32×10^5	18.9
2	9.30×10^8	4100	4.90×10^5	3.4
3	6.90×10^9	9000	7.20×10^5	1

the steel vessel is separated from the HE charge by a foam cushioning region or a standoff space, either evacuated or filled with gas at modest pressure. The possibility of constructing a reusable device using high explosives is supported by the work of Refs. 14 and 15. The investigators of these references were able to reuse a heavy hemispherical steel chamber in which 2 to 6 mm of PETN was detonated in contact with the chamber wall (or in contact with a copper liner that was, in turn, in contact with the wall). There are a number of advantages of reusable HE driven pump tube. If it can be made sufficiently reliable, it can become a very compact, low-mass laboratory tool (relative to a conventional pump tube), which operates without destroying its immediate surroundings. No large blast chamber would be required and instrumentation could be placed close to the pump tube.

Table 8 shows the state points for a proposed high-explosive driven pump tube cycle. The working gas is ideal hydrogen with a specific heat ratio of 1.4, the initial temperature is 300 °K, the maximum cycle pressure is 6.90×10^9 dynes/cm^2, and no losses are considered. (These are the same assumptions used to calculate the pump tube cycles of Sec. II.) The first state point is the initial fill condition, the second is after the initial shock and the third is after the reflected shock. The HE was assumed to be PBX 9404. The piston velocity (=detonation velocity) was taken from Ref. 16 as 8.77 km/s. If we compare this cycle with the cycle for the conventional (single compression) pump tube (Table 2, Sec. II), two important points can be noted. First, the HE driven cycle produces temperatures and sound speeds which (ideally) exceed those of the conventional cycle. Second, the maximum pump tube volume of the former is only 0.083 times that of the latter. To see to what extent this relatively very small pump tube volume of the high-explosive driven device can translate into a smaller and lighter complete pump tube (including pressure vessel), a preliminary design is performed in the following paragraphs.

As a benchmark, we again use the NASA Ames 2.54 cm gun (see Table 1, Sec. II). We keep the pump tube diameter fixed at 10.16 cm and reduce the pump tube length by the factor of 0.083 quoted earlier. The high-explosive driven pump tube length thus becomes 191 cm. From the volume of the chamber and the gas properties of Table 8, we can calculate the mass of gas required (15.4 g) and the energy required to raise it from the initial to the final temperature (1.39×10^{13} erg). In Ref. 17, the properties of PBX 9404 are given in some detail. Equation-of-state data for HE products can be found in the SESAME equation-of-state library,[18] prepared by the Los Alamos Scientific Laboratory. Using the above data and the one-dimensional conservation equations of mass, momentum and energy, the energy released by PBX 9404 can be calculated to be 0.813×10^{11} ergs/g. Assuming an efficiency of transfer of energy from the HE to the working gas of 10% (see Ref. 11), the mass of HE required is 1710 g; since the density of the HE is 1.84 g/cm^3, the volume of HE required in 925 cm^3. We assume that the liner is magnesium and that the maximum inward velocity of the liner is 1.0 km/s. We further assume that 1/3 of the detonation energy of the HE can be transferred to kinetic energy of the liner. With these assumptions, the liner mass and volume can be calculated to be 9250 g and 5440 cm^3, respectively. A simple geometrical calculation then yields the thickness of the liner and HE annular zones, which are 0.88 cm and 0.130 cm, respectively.

From Ref. 16, the detonation failure diameter of PBX 9404 is 0.118 cm, not very far below the required thickness of our annular HE zone. However, in our geometry, the HE is better tamped, both because of a nearly one-dimensional (planar) geometry vs the two-dimensional (cylindrical) geometry in the detonation failure diameter tests and because of the liner, initially on one side of the HE. Hence, PBX 9404 in our geometry should be able to propagate a detonation wave properly. If problems of detonation failure were to occur, one could switch from a HMX-based HE (i.e., PBX 9404) to a PETN-based HE, which could be much more sensitive and have a much smaller detonation failure diameter.

The standoff distance between the inside of the pressure vessel and the HE necessary to reduce the pressure of the HE products sufficiently to allow the pressure vessel to be reusable is estimated as follows. The pressure and density of PBX 9404 immediately after detonation can be obtained from data given in Ref. 17. Isentropic and constant energy expansions are then made from this state point, using SESAME equation-of-state (EOS) data[18] for the HE products. The HE products are assumed to expand isentropically in the axial direction from the detonation conditions back to zero velocity and the initial (before detonation) density. The products are then assumed to expand at constant internal energy out to the pressure vessel wall. During this expansion, linear motion is neglected, which is conservative. The HE products are allowed to expand volumetrically by a factor of 17.4. The inside diameter of the pressure vessel then follows directly and is 15.71 cm. Using the SESAME EOS data as described above yields a HE products pressure after (both) expansions of 2.04×10^9 dynes/cm^2. No attempt is made here to allow in detail for the unsteady loading of the pressure vessel. Rather, the pressure vessel is designed based on static loading at twice the HE products pressure estimated above.

From Ref. 10, 4140 steel heat treated to a Brinell hardness of 370 has a yield strength of 1.14×10^{10} dynes/cm^2 and an elongation of 13%, thus still retaining significant ductility. We will operate at 80% of this value, or 9.10×10^9 dynes/cm^2. The ratio of the working tensile stress to the assumed effective static load pressure is thus $9.10 \times 10^9/(2 \times 2.04 \times 10^9) = 2.23$. From Ref. 19, the ratio of the outside-to-inside diameter necessary to produce the above stress ratio is 1.62. The necessary outside diameter of the pressure vessel is thus 25.5 cm. The total pump tube length required is increased from the basic value of 191 cm by 10.1 cm to allow for the volume of the final, doubly compressed gas (see normalized volumes of Table 8), and by one outside diameter, 25.5 cm, to allow for the two end closures. The total outside length of the pump tube is thus 226 cm. This is 11.1 times less than the length of the benchmark conventional pump tube of the NASA Ames 2.54 cm gun. To estimate the mass of the pump tube for the HE driven case, the effective tube length is increased by another outside diameter, 25.5 cm, to allow for threaded end closure sleeves, etc., to allow the tube to be opened at both ends. The pump tube mass can then readily be estimated to be 6.18×10^5 g. This is 7.06 times less than that of the benchmark conventional pump tube. Thus, very considerable reductions in pump tube length and mass are, in principle, possible through the use of the HE driven pump tube technique.

The concept of this section has some potential for increase in the achievable sound speed, according to the higher sound speeds calculated in Table 8 vs those of Table 2. However, there are a number of arguments (discussed in detail in Sec. II with respect to the concept presented in that section) that indicate it may be very difficult to achieve, in practice, anything close to the sound speed gains calculated by simple analyses neglecting losses. Because of the difficulty of calculating the degree of sound speed increases achievable in practice, allowing for losses, using the concept of this section, we confine ourselves here to simply stating that the potential exists.

VI. Conclusions

In a pump tube, a gas is mechanically compressed, producing very high pressures and sound speeds. The intensely heated gas produced in such a tube can be used to drive light gas guns and shock tubes or shock tunnels. Three concepts have been presented that have the potential to allow substantial reductions in the size and mass of the pump tubes to be achieved. Also, they may allow modest but useful increases in sound speed to be achieved. All of the size and mass reductions and performance increases have been referenced to a benchmark conventional piston-driven pump tube. The first concept involves the use of one or more diaphragms in the pump tube, thereby replacing a single compression process by two or more successive compression processes. Results have been presented indicating that pump tube lengths can be reduced by factors of 3 to 4 in this way, while achieving the same sound speed. Results for a different type of pump tube configuration have been presented indicating that, using the same size pump tube, projectile velocities in light gas guns could be increased by 40% to 90%, using pump tube diaphragms, if losses are neglected. Loss mechanisms are discussed that are likely to greatly reduce these latter gains. The sizing and operation of the necessary pump tube diaphragms has been analyzed. It was concluded that the necessary diaphragm dimensions were quite reasonable and the diaphragms could open quickly enough to allow free passage of the pump tube piston.

The second concept presented involves a large reduction in the length-to-diameter ratio of the pump tube and the piston. It was shown that the length of the pump tube could be decreased by a factor of ~ 8 using this concept, although the mass of the pump tube will remain relatively unchanged.

The last concept presented involves the shock heating of the working gas using high explosive in a cylindrically symmetric geometry. This is a reusable version of an expendable, one-shot high-explosive driven pump tube concept used earlier by other workers. A preliminary design analysis was presented indicating that the pressure vessel stresses can be kept sufficiently low so that the reusable device should be feasible. It was shown that reductions in pump tube length and mass by factors of ~ 11 and ~ 7, respectively, should be achievable using this concept. This concept also has some potential for increase in the sound speed achievable. Loss mechanisms may limit the degree to which this potential gain may be achieved in practice.

References

[1]Seigel, A. E., "The Theory of High Speed Guns," AGARDograph 91, May 1965.

[2]Canning, T. N., Seiff, A., and James, C. S., eds., "Ballistic Range Technology," AGARDograph 138, Aug. 1970.

[3]Canning, T. N., Seiff, A., and James, C. S., eds., "Ballistic Range Technology," AGARDograph 138, Aug. 1970, pp. 41–44.

[4]Miller, R. J., private communication, Feb. 1988.

[5]Canning, T. N., Seiff, A., and James, C. S., eds., "Ballistic Range Technology," AGARDograph 138 Aug. 1970, p. 79.

[6]Seigel, A. E., "The Theory of High Speed Guns," AGARDograph 91, May 1965, p. 227.

[7]Knowlen, C., private communication, Feb. 1988.

[8]Canning, T. N., Seiff, A., and James, C. S., eds., "Ballistic Range Technology," AGARDograph 138, Aug. 1970, p. 149.

[9]Voitenko, A. E., "Generation of High-Speed Gas Jets," *Soviet Physics Doklady*, Vol. 9, No. 10, April 1965, pp. 860–862.

[10]*ASM Metals Reference Book*, 2nd ed., American Society for Metals, Metals Park, OH, 1983, p. 214.

[11]Gill, S. P. and Simpkinson, W. V., "Analysis and Performance of an Explosively Driven Shock Tube," *Proceedings of the 7th International Shock Tube Symposium*, Toronto, Canada, University of Toronto Press, Toronto, Canada, June 1969, pp. 366–395.

[12]Crosby, J. K., Gill, S. P., and Fowles, G. R., "Explosive Compression of Helium for Hypervelocity Applications," *Fourth Hypervelocity Techniques Symposium,* Arnold Air Force Station, TN, Denver Research Institute, Denver, CO, Nov. 1965, pp. 429–456.

[13]Moore, E. T., Mumma, D., Godfrey, C. S., and Bernstein, D., "Explosive Gas Guns for Hypervelocity Acceleration," *Fourth Hypervelocity Techniques Symposium*, Arnold Air Force Station, TN, Nov. 1965, pp. 457–484.

[14]Flagg, R. F. and Glass, I. I., "Explosive-Driven, Spherical Implosion Waves," *Physics of Fluids*, Vol. 11, Oct. 1968, pp. 2282–2284.

[15]Glass, I. I. and Sagie, D., "Application of Explosive-Driven Implosions to Fusion," *Physics of Fluids*, Vol. 25, Feb. 1982, pp. 269–270.

[16]Gibbs, T. R. and Popolato, A., eds., "LASL Explosive Property Data," Univ. of California Press, Berkeley, CA, 1980, p. 235.

[17]Gibbs, T. R. and Popolato, A., eds., "LASL Explosive Property Data," Univ. of California Press, Berkeley, CA, 1980, pp. 84–98.

[18]Cooper, N. G., ed., "An Invitation to Participate in the LASL Equation of State Library," Los Alamos Scientific Laboratory Report LASL-79-62, 1980.

[19]Popov, E. F., *Mechanics of Materials*, 2nd ed., Prentice-Hall, Englewood Cliffs, NJ, 1978, pp. 557–564.